JOURNAL OF SPACECRAFT AND ROCKETS
Vol. 30, No. 5, September–October 1993

Six-Degree-of-Freedom Guidance and Control-Entry Analysis of the HL-20

Richard W. Powell*
NASA Langley Research Center, Hampton, Virginia 23681

The ability of the HL-20 lifting body to fly has been evaluated for an automated (no pilot inputs) entry from atmospheric interface to landing. This evaluation was required to demonstrate that not only successful touchdown conditions would be possible for this low lift-to-drag-ratio vehicle (≅4), but also the vehicle would not exceed its design dynamic pressure limit of 400 psf during entry. This dynamic pressure constraint limit, coupled with limited available pitch-control authority at low supersonic speeds, restricts the available maneuvering capability for the HL-20 to acquire the runway. One result of this analysis was that this restrictive maneuvering capability does not allow the use of a model-following atmospheric entry-guidance algorithm, such as that used by the Space Shuttle, but instead requires a more adaptable guidance algorithm. Therefore, for this analysis, a predictor-corrector guidance algorithm was developed that would provide successful touchdown conditions while not violating the dynamic pressure constraint. A flight-control system was designed and incorporated, along with the predictor-corrector guidance algorithm, into a six-degree-of-freedom simulation. This simulation was tested under many combinations of off-nominal atmospheric density profiles and winds and showed that the HL-20 remained controllable. This simulation also indicated that the HL-20 could reach the landing site and execute a successful landing under all off-nominal conditions simulated.

Nomenclature

$\bar{c}$	= reference chord, ft
C_{m0}	= pitching-moment coefficient at zero α, n.d.
C_m	= pitching-moment coefficient (pitching moment/$\bar{q}S\bar{c}$), n.d.
h	= altitude, ft
p	= roll rate, deg/s
p_c	= commanded roll rate, deg/s
q	= pitch rate, deg/s
$\bar{q}$	= dynamic pressure, psf
r_{stab}	= stability-axis yaw rate, deg/s
S	= reference area, ft^2
U_{xc}	= commanded number of roll RCS thrusters (+ roll right)
U_{yc}	= commanded number of pitch RCS thrusters (+ pitch up)
U_{zc}	= commanded number of yaw RCS thrusters (+ yaw right)
$V_{E\text{-}W}$	= East-West wind velocity, ft/s
$V_{N\text{-}S}$	= North-South wind velocity, ft/s
α	= angle of attack, deg
α_c	= commanded angle of attack, deg
β	= sideslip angle, deg
δ_a	= aileron deflection, deg
δ_e	= elevator deflection, deg
δ_r	= rudder deflection, deg
δ_{sb}	= speed brake deflection, deg
γ	= flight-path angle, deg
ρ	= atmospheric density, slug/ft^3
ρ_{76}	= 1976 standard atmospheric density, slug/ft^3
ϕ	= roll angle, deg
ϕ_c	= commanded roll angle, deg
σ	= standard deviation
$\Delta\alpha$	= maximum deviation in angle of attack from nominal for 1.5<Mach<2.0, deg

Received Dec. 10, 1992; revision received Jan. 15, 1993; accepted for publication Jan. 28, 1993.

*Aerospace Engineer, Vehicle Analysis Branch, Space Systems Division.

Introduction

ONE of the main issues that had to be resolved before declaring the HL-20 a viable candidate for the personnel launch system was to demonstrate safe, reliable entries to a runway landing after deorbit burn. There are two major areas of concern: namely, 1) successful landing after unpowered entry, and 2) pitch control at low-supersonic speeds. The landing issue comes about because of the HL-20's low subsonic lift-to-drag ratio. Because the HL-20 is designed to be operated both automatically and piloted, a pilot-in-the-loop simulation was developed specifically to address this landing issue, and the results are reported in Ref. 1. The automatic capability from acquisition of the atmospheric interface to touchdown is described in this paper. The second issue can best be explained by the examination of aerodynamic data.[2] At low supersonic speeds, the pitching-moment coefficient at 0-deg angle of attack, C_{m0}, is negative such that the available control surfaces can provide a flyable corridor width of only 4-deg angle of attack α. The upper end of this boundary is defined by the available pitch-up control, and the lower limit is the minimum α which ensures that the HL-20 will not exceed the design dynamic pressure limit.

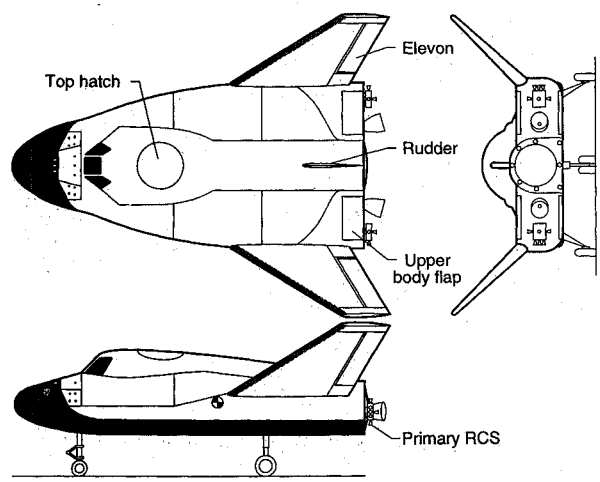

Fig. 1 HL-20.

Because of this narrow corridor, a guidance system must be designed that both minimizes the range/altitude errors at these low supersonic speeds and, thus, limits the required α modulation, while providing the required state conditions for the landing guidance phase.

The initial guidance algorithm[3] was designed before the loads capacity analysis was complete. This algorithm used a model-following technique similar to that used by the Space Shuttle (the vehicle is commanded to fly to a predetermined profile) until the initiation of the landing phase. This technique gradually reduced the allowable errors in range/altitude until the initiation of the landing phase. However, when the low-supersonic-speed constraints were added, this algorithm was unable to fly in the allowable corridor under all simulated off-nominal conditions. Because of the combination of constraints, the guidance algorithm was reformulated from a model-following to include a state-of-the-art predictor-corrector algorithm. The predictor-corrector algorithm is a three-degree-of-freedom formulation using numerically derived sensitivities designed to provide successful landing initiation, while meeting low supersonic angle-of-attack limitations. This predictor-corrector algorithm was incorporated within the guidance algorithm of the six-degree-of-freedom simulation.

This paper describes the six-degree-of-freedom simulations used to demonstrate the flyability of the HL-20. Included is a description of the flight-control system, design and implementation of the guidance algorithm, and off-nominal conditions used for evaluation.

Table 1a HL-20 characteristics used in entry simulation, mass and dimensions

Weight, lb	19,100
Length, ft	28.24
Wing span, ft	13.89
Reference area, ft^2	286.45
I_{xx}, slug-ft^2	7512
I_{yy}, slug-ft^2	33,594
I_{zz}, slug-ft^2	35,644

Table 1b HL-20 characteristics used in entry simulation reaction-control system characteristics

Axis	Thruster force, lb	Thruster moment, ft-lb	Number of thrusters commanded
Roll	25	100	2, 4
Pitch	25	333	2, 4
Yaw	25	333	1, 2, 3

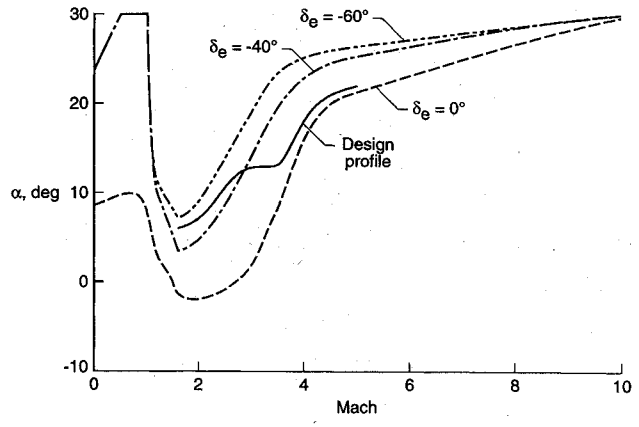

Fig. 2 Trim α capability of HL-20.

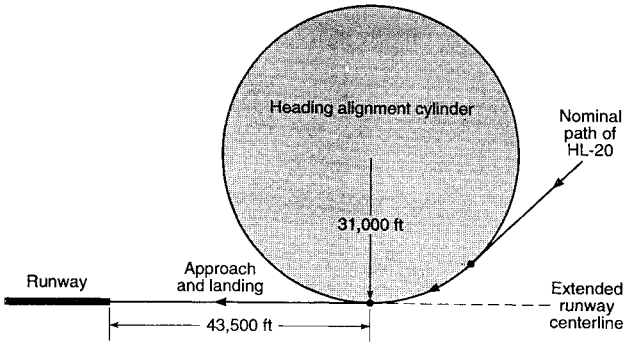

Fig. 3 HAC geometry.

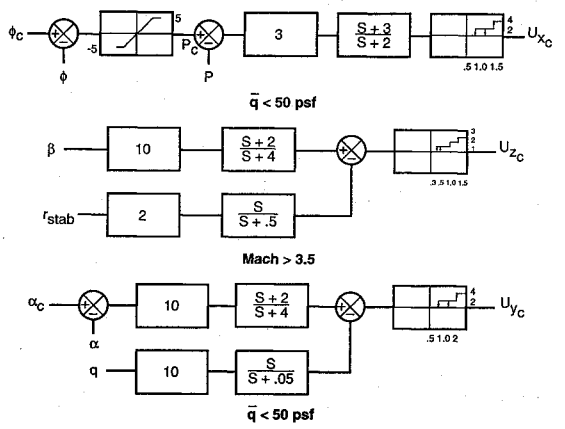

a) Reaction-control system

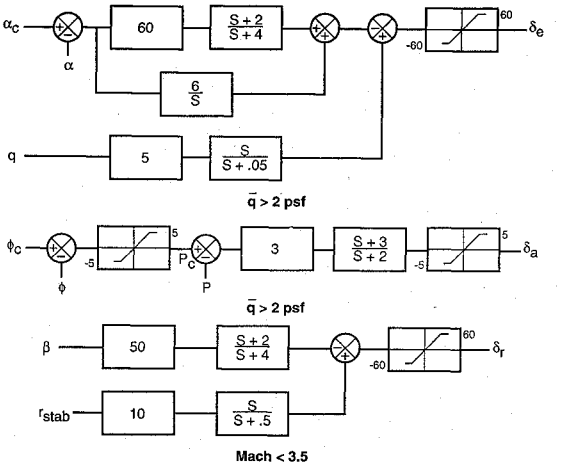

b) Aerodynamic surfaces

Fig. 4 HL-20 flight control system.

Vehicle Description

Figure 1 shows the HL-20 vehicle and indicates the location of the aerodynamic controls and reaction-control system used during entry. The vehicle has seven aerodynamic control surfaces: namely, two upper body flaps, two lower body flaps, two elevons located on the fins, and a rudder. In addition, the HL-20 has a three-axis reaction-control system (RCS) located on the base of the vehicle. The mass properties and RCS characteristics used in the simulations are shown in Table 1.

Aerodynamics

The aerodynamics used for the simulations are described in Ref. 2. Figure 2 shows the trim angle of attack with zero control deflec-

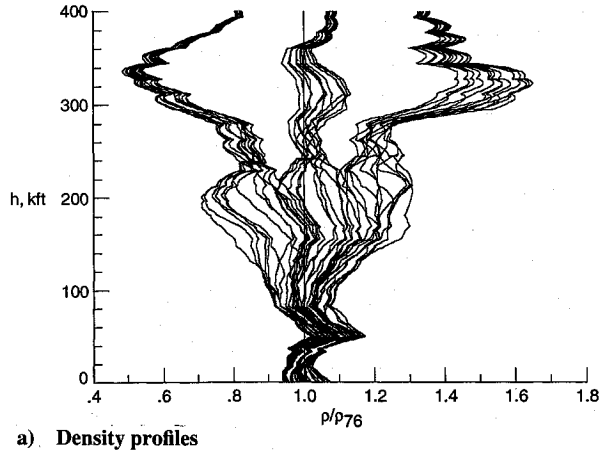

a) Density profiles

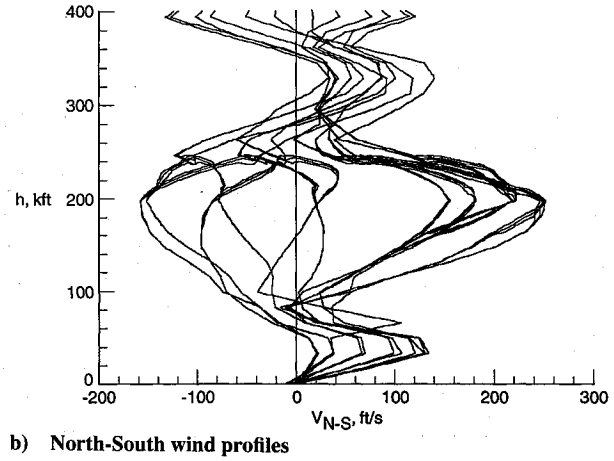

b) North-South wind profiles

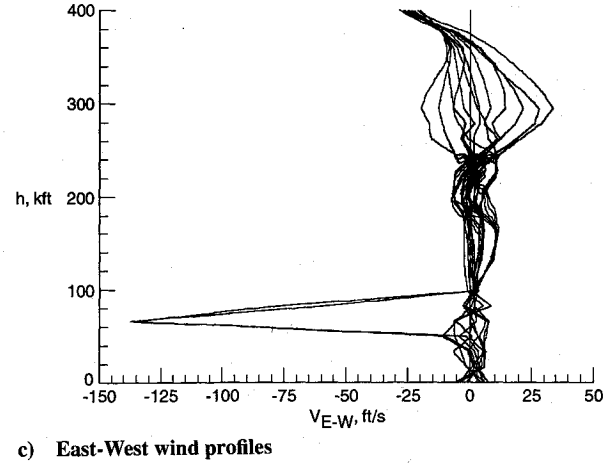

c) East-West wind profiles

Fig. 5 Atmospheric density and wind profiles used in simulation.

tions as a function of Mach number. As can be seen from the figure, the vehicle would trim at negative angles of attack without control deflections at low supersonic speeds. This figure also shows the trim α history possible by using both the elevons and upper body flaps. In addition, the nominal α history used by the guidance algorithm is depicted. This nominal α history was chosen to maintain the dynamic pressure within acceptable limits (less than 400 psf), while also providing a ±2-deg control margin.

Guidance Algorithm

The entry-guidance algorithm for the HL-20 is divided into three major phases: entry, terminal area, and landing. Each major

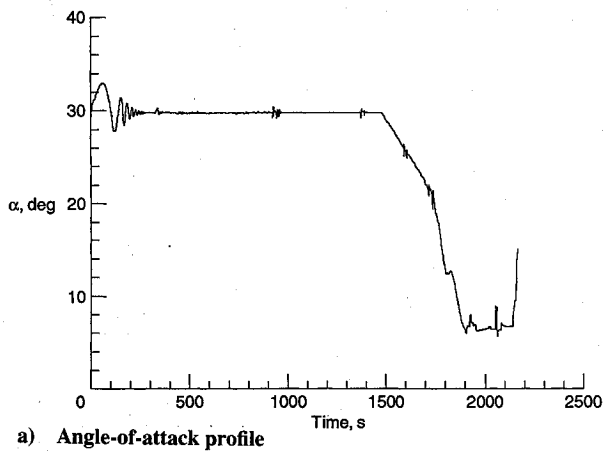

a) Angle-of-attack profile

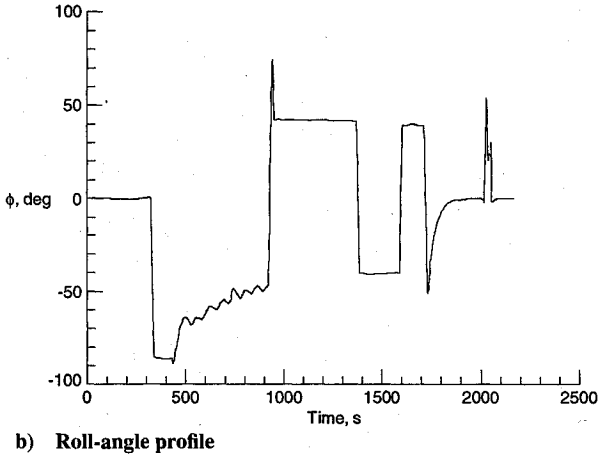

b) Roll-angle profile

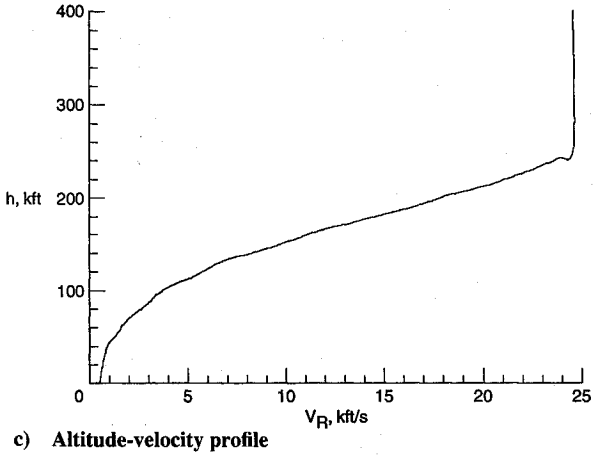

c) Altitude-velocity profile

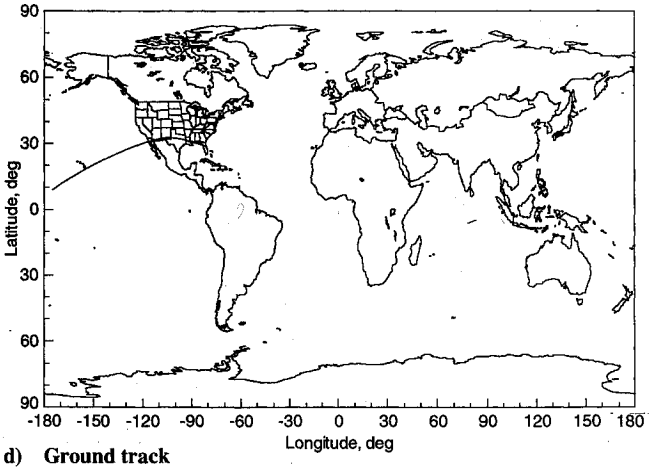

d) Ground track

Fig. 6 Nominal entry of HL-20.

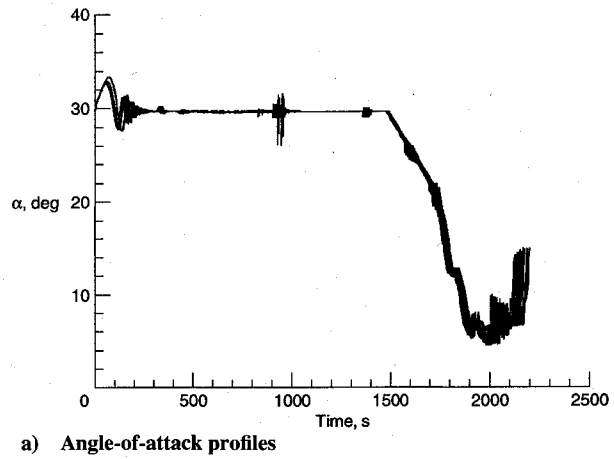

a) Angle-of-attack profiles

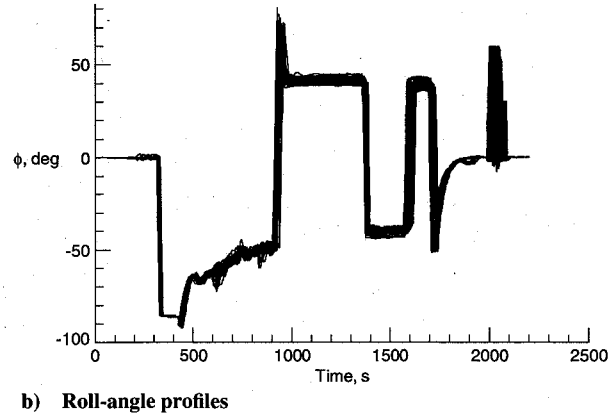

b) Roll-angle profiles

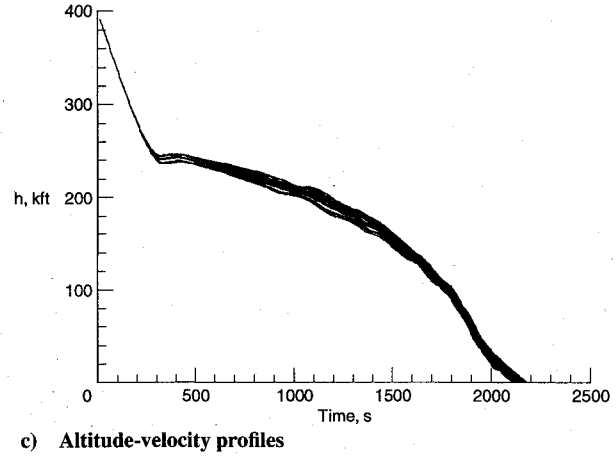

c) Altitude-velocity profiles

Fig. 7 Profiles of entries from atmospheric interface to touchdown in presence of off-nominal atmospheric conditions.

phase is further divided into subphases. Table 2 outlines the guidance strategy, with more detailed description given next.

The entry phase is divided into three subphases. The first is active from atmospheric interface (assumed in these simulations to be 400k ft) until pullout (γ=0 deg). During the entire entry phase, the guidance commands the vehicle to fly the α that would result if all controls were undeflected. Also, during the entry-guidance phase, the roll direction is determined from the error in heading angle. If the heading-angle error (difference between the vehicle's current heading and that toward the runway) is greater than 10 deg, the vehicle is commanded to perform a roll reversal. During the first subphase, the roll angle is commanded to be zero until the reference stagnation heating rate increases to 55% of the desired pullout value. At this time, the vehicle is commanded to roll to the nominal angle required to maintain the desired heating rate after pullout. This roll maneuver in anticipation of pullout smooths the required vehicle motions at pullout. During the second subphase, the vehicle is commanded to roll to maintain the desired heating rate. Once the Mach number has been reduced to 20, the predictor-corrector guidance algorithm is activated.

The predictor-corrector algorithm in the entry phase determines the constant roll-angle magnitude that would be required to reach the initiation of the landing phase while flying the nominal α profile. When this roll-angle magnitude is less than the roll angle required to maintain the constant heating rate, the final subphase is entered. If the roll-angle magnitude determined by the predictor-corrector algorithm is greater than that required to maintain the constant heat rate, the vehicle is commanded to remain on the desired heat-rate boundary. (If the HL-20 were to roll to the predictor-corrector value, the heating rate would increase above the desired value.)

The final entry-guidance subphase is the terminal-area acquisition phase. During this phase, the HL-20 uses the roll-angle magnitude as determined by the predictor-corrector algorithm. For these simulations, the predictor-corrector algorithm was interrogated at 30-s intervals. This update frequency has not been optimized.

Once the HL-20's Mach number has been reduced to 5, the terminal-area guidance phase is entered. This guidance phase is composed of two subphases. The first directs the HL-20 from Mach 5 to the interception of the heading alignment cylinder (HAC). The HAC is an imaginary cylinder tangential to the runway with a radius of 31,000 ft located 43,500 ft from the beginning of the runway. The HAC geometry is shown in Fig. 3. The second subphase determines the roll-angle history that is required to maintain the HL-20 on the HAC. The HAC radius determines the nominal roll angle, and the distance from the runway determines the outer-glide-slope angle. For the HL-20, a 20-deg nominal bank angle was baselined for the HAC, along with a nominal outer-glide-slope flight-path angle of -19 deg. This outer-glide slope angle allows

Table 2 HL-20 Entry guidance algorithm characteristics

Guidance phase	Guidance subphase	Subphase characteristics
Entry	Atmospheric Interface to pullout	α_c is undeflected control's static value. ϕ_c used to control pullout at proper heat rate/ roll reversals used to control heading angle.
Entry	Constant heat rate	α_c is undeflected control's static value. ϕ_c modulated to maintain desired heat rate/ roll reversals used to control heading angle.
Entry	TAEM acquisition	α_c is undeflected control's static value. ϕ_c determined from predictor-corrector algorithm/roll reversals used to control heading angle.
TAEM	HAC acquisition	α_c determined from predictor-corrector algorithm. ϕ_c used to control heading angle directly.
TAEM	HAC	α_c determined from predictor-corrector algorithm. f_c used to remain on HAC.
Landing	Transition to outer glide slope	α_c transition from HAC to outer glide slope. ϕ_c used to control heading. δ_{sb} speed brake commanded to control $\bar{q}$.
Landing	Outer glide slope	α_c required to remain on glide slope. ϕ_c used to control heading. δ_{sb} speed brake commanded to control $\bar{q}$.
Landing	Flare maneuver 1	α_c required for flare. ϕ_c used to control heading. δ_{sb} retracted.
Landing	Flare maneuver 2	α_c required for flare. ϕ_c used to control heading. δ_{sb} retracted.
Landing	Energy depletion	α_c required for proper touchdown. ϕ_c used to control heading. δ_{sb} retracted.

Table 3a Touchdown conditions for HL-20 encountering off-nominal atmospheric density profiles and winds

		January			February			March			April		
	Nominal	−3σ[a]	Mean[b]	+3σ[c]	−3σ	Mean	+3σ	−3σ	Mean	+3σ	−3σ	Mean	+3σ
a_{td}, deg	15.0	14.2	14.4	14.6	14.2	14.4	14.7	14.2	14.4	14.6	14.3	14.5	14.7
V_{td}, ft/s	346	367	356	345	366	353	342	365	354	343	360	350	342
x_{td}, ft	2203	2633	2449	2265	2647	2396	2215	2658	2437	2243	2582	2410	2260
$\dot{h}_{td}$, ft/s	−4.0	−3.8	−3.9	−4.0	−3.8	−3.9	−4.0	−3.9	−3.9	−4.0	−3.8	−3.9	−4.0
Δα, deg	0.12	0.27	0.24	0.50	0.30	0.47	0.60	0.20	0.36	0.59	0.18	0.63	0.44

[a]−3α=GRAM−3α density perturbations with means winds for specified month.
[b]Mean=GRAM mean density and winds for specified month.
[c]+3α=GRAM+3α density perturbations with means winds for specified month.

Table 3b Touchdown conditions for HL-20 encountering off-nominal atmospheric density profiles and winds

	May			June			July			August		
	−3σ	Mean	+3σ	−3σ	Mean	+3σ	−3σ	Mean	+3σ	−3σ	Mean	+3σ
a_{td}, deg	14.5	14.7	14.9	14.7	14.8	15.0	14.7	14.8	14.9	14.7	14.8	14.9
V_{td}, ft/s	354	347	339	352	347	341	354	349	344	354	349	345
x_{td}, ft	2484	2335	2181	2382	2315	2176	2431	2309	2241	2417	2316	2240
$\dot{h}_{td}$, ft/s	−3.9	−3.9	−4.0	−3.9	−3.9	−4.0	−3.9	−3.9	−4.0	−3.9	−3.9	−4.0
Δα, deg	0.07	0.30	0.30	0.15	0.17	0.18	0.14	0.19	0.36	0.28	0.32	0.27

Table 3c Touchdown conditions for HL-20 encountering off-nominal atmospheric density profiles and winds

	September			October			November			December		
	−3σ	Mean	−3σ	−3σ	Mean	−3σ	−3σ	Mean	−3σ	−3σ	Mean	−3σ
a_{td}, deg	14.8	14.8	14.9	14.5	14.6	14.9	14.3	14.5	14.7	14.2	14.4	14.6
V_{td}, ft/s	351	347	343	357	349	340	363	352	343	365	355	346
x_{td}, ft	2308	2307	2235	2482	2363	2173	2617	2387	2230	2627	2724	2278
$\dot{h}_{td}$, ft/s	−3.9	−3.9	−4.0	−3.9	−3.9	−4.0	−3.9	−3.9	−4.0	−3.8	−3.9	−4.0
Δα, deg	0.34	0.35	0.73	0.31	0.22	0.42	0.30	0.23	0.55	0.27	0.30	0.69

for effective speed brake control and provides sufficient energy for the flare maneuver. The landing phase is initiated when the HL-20 is aligned with the runway centerline. The predictor-corrector guidance algorithm was employed in both subphases. The predictor-corrector guidance algorithm was used to determine the bias to the nominal angle-of-attack profile that was necessary to initiate the landing phase at the proper altitude. The roll angle during the HAC intercept phase was the roll angle (sign and magnitude) required for successful intercept. Once the HAC was intercepted, the roll angle was modulated to remain on the HAC. The predictor-corrector update frequency was increased to every 10 s once the Mach number was reduced to 3.

After the HL-20 intercepted the runway centerline, the guidance algorithm entered the landing phase. During this phase, no predictor-corrector logic was employed. The landing guidance phase was divided into five subphases. During the entire landing phase, the roll angle is commanded to fly the HL-20 to the runway centerline. Until the first flare maneuver (subphase 3), the speed brake is commanded to maintain a dynamic pressure of 300 psf. The first subphase is of 20-s duration and is used to transition from the flight-path angle at the end of the terminal-area guidance phase to that required to fly the outer glide slope (subphase 2) by linearly ramping in the error in the flight-path angle. At the end of subphase 1, the HL-20 enters subphase 2, or outer-glide-slope phase. During this phase, the HL-20 modulates the flight-path angle to nominally touch down 2200 ft down the runway after flaring. The third subphase is initiated at an altitude of 2000 ft, and the fourth at an altitude of 137 ft. The third and fourth subphases generate α commands to perform a double parabolic flare maneuver designed such that the HL-20 is at level flight at an altitude of 10 ft. The fifth subphase is initiated at this point and designed to bleed off excess energy such that the HL-20 will nominally touch down at 205 knots, with a vertical velocity less than 5 ft/s, and at an α less than 15 deg.

Flight-Control System

The HL-20 is controlled during entry by a combination of aerodynamic surfaces and a three-axis reaction control system (RCS). The pitch and roll RCS are active until the dynamic pressure increases to 50 psf, whereas the yaw RCS remains active until the Mach number is reduced to 3.5. All aerodynamic surfaces, with the exception of the rudder, become active when the dynamic pressure reaches 2 psf, and the rudder becomes active when the Mach number is reduced to 3.5. The control system was designed by using the elevons for pitch control augmented by the upper body flaps, the lower body flaps for roll control, the rudder for yaw control, and the upper and lower body flaps for speed brake. The speed brakes are used to limit dynamic pressure to 300 psf when the HL-20 is flying the outer-glide-slope portion of the landing guidance phase. Figure 4 shows the control system. Note that this control-system design has no gain scheduling or switching logic. The control system for the HL-20 is relatively simple because the vehicle is directionally stable during the entire entry. This control system was designed in the s plane, and converted to the z plane using the convolution technique.[4]

Atmospheric Profile Modeling

Off-nominal atmospheric conditions, both density dispersions and wind profiles, were used within the six-degree-of-freedom simulations. The nominal entry profile was determined using the 1976 U.S. standard atmosphere.[5] Density and wind profiles were generated using the global reference atmosphere model (GRAM)[6] to simulate realistic variations in atmospheric conditions. The GRAM was developed to provide realistic worldwide atmospheric data including winds. It was used to generate the monthly mean density, wind profiles, and standard deviation data for the density profiles. A total of 37 simulations of the complete entry from atmospheric interface (400k ft) to touchdown were generated. These

were as follows: 1) U.S. 1976 Standard Atmosphere with no winds, 2) monthly mean data with winds, and 3) $\pm 3\ \sigma$ monthly density data with mean monthly winds. These density and wind profiles are shown in Fig. 5.

Generally to complete a study of this type, turbulence and the effect of head and crosswinds during the landing phase should be considered. These effects have been examined extensively with the pilot-in-the-loop simulations[1] for the HL-20 and will not be examined in this paper. The main intent of the study was to demonstrate that safe and controllable landings are possible in the presence of off-nominal conditions, even with the limited α-control margin in the low supersonic flight regime.

Design Mission

The design mission was an entry from the Space Station Freedom to the Space Shuttle runway at the NASA Kennedy Space Center. The particular orbit chosen only required 170 n.mi. of crossrange to reach the runway. This choice, which is less than 20% of the capability of the HL-20, requires more roll maneuvering than a larger crossrange entry, and thus should be more taxing on the control (more aerodynamic surface movement and RCS usage) and guidance algorithms (more difficult heading control). Figure 6 shows the design entry as a ground track as well as entry histories of α, ϕ, and h. Note that the HL-20 is commanded to fly a preprogrammed α profile until the velocity is reduced to Mach 5. For velocities below Mach 5, α is used to control range. Until the velocity is reduced to Mach 5, ϕ is used to control the heating rate, range, and heading error. Below Mach 5, ϕ is used to control heading error.

Simulation Results

The profiles showing the entry simulations from the atmospheric interface (400k ft) to touchdown are given in Fig. 7, and a summary of the conditions at touchdown is given in Table 3. These simulations were generated by simulating off-nominal density profiles and winds. The entry profiles of Fig. 7 show the wide range of entry profiles resulting from these off-nominal conditions. Table 2 shows that all these trajectories were successful using the following criteria: 1) The required a modulation between Mach 1.5 and 2.0 is less than +2 deg ($\Delta\alpha$) from the nominal; 2) all touchdown α were less than 16 deg (scrape angle = 20 deg); 3) the touchdown distances were within ± 400 ft of the design condition of 2200 ft; and 4) the descent rate $\dot{h}$ was less than 5 ft/s (design limit = 10 ft/s). The net result from these simulations and those from the piloted-in-the-loop studies is that the HL-20 can be safely landed under a wide variety of off-nominal conditions without violating any vehicle constraints.

Conclusions

A study has been conducted to evaluate the automated entry of the HL-20 from atmospheric interface to touchdown. Because of the small flyable angle-of-attack range at low supersonic speeds (combination of limited pitch-up control authority and design dynamic pressure constraint), a Space-Shuttle-type model-following guidance routine was inadequate for the task. Therefore, a predictor-corrector guidance algorithm was developed to guide the vehicle from Mach 20 to the initiation of the landing phase to insure that this in-flight dynamic pressure constraint was not violated and still provide for a successful landing. A control system was also developed and implemented along with the guidance algorithm into a six-degree-of-freedom simulation. Six-degree-of-freedom simulations were conducted that demonstrated the capability of this vehicle to successfully execute an entry and landing event when encountering off-nominal atmospheric conditions.

References

[1]Jackson, E. B., Ragsdale, W. A., and Powell, R. W., "Utilization of Simulation Tools in the HL-20 Conceptual Design Process," AIAA Paper 91-2955, Aug. 1991.

[2]Jackson, E. B., Cruz, C. I., and Ragsdale, W. A., "Real-Time Simulation Model of the HL-20 Lifting Body," NASA TM 107580, July 1992.

[3]Powell, R. W., and Cruz, C. I., "Guidance and Control Analysis of the Entry of a Lifting Body Personnel Launch Vehicle," AIAA Paper 91-0055, Jan. 1991.

[4]Kaylor, J. T., Rowell, L. F., and Powell, R. W., "A Real-Time Digital Computer Program for the Simulation of Automatic Spacecraft Reentries," NASA TM X-3496, July 1977.

[5]"U.S. Standard Atmosphere, 1976," National Oceanic and Atmospheric Administration, NASA and U.S. Air Force, Washington, DC, Oct. 1976.

[6]Justus, C. G., Fletcher, G. R., Gramlina, F. E., and Pace, W. B., "The NASA/MSFC Global Reference Atmospheric Model—Mod 3 (with Spherical Harmonic Wind Model)," NASA CR 3256, 1980.